Environmental Pollution 357 (2024) 124362



Contents lists available at ScienceDirect

Environmental Pollution

journal homepage: www.elsevier.com/locate/envpol

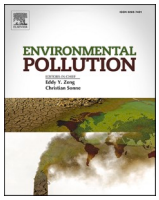



Year-round spatial and temporal distribution of microplastics in water and sediments of an urban freshwater system (Jungnang Stream, Korea)☆

Dat Thanh Pham [a,b], Sang-Hyun Choi [b], Jung-Hwan Kwon [b,*]

[a] BK21 FOUR R&E Center for Environmental Science and Ecological Engineering, Korea University, Seoul, 02841, Republic of Korea
[b] Division of Environmental Science and Ecological Engineering, Korea University, 145 Anam-ro, Seongbuk-gu, Seoul, 02841, Republic of Korea

ARTICLE INFO

Keywords:
Microplastics
Freshwater
Stream
Distribution
Annual load

ABSTRACT

Streams and tributaries can play a significant role in the transport of inland microplastics to rivers and oceans; however, research on microplastics in these water bodies is limited compared to riverine and marine environments. Analyzing microplastic abundance at higher spatial and temporal resolutions is crucial to comprehend the dynamics of microplastics in these water bodies. Therefore, this study investigated year-round spatiotemporal variations of microplastics monthly in surface waters and sediments along the Jungnang Stream, one of the main tributaries to the Han River in South Korea. The mean concentration of microplastics in the stream was 9.8 ± 7.9 particles L^{-1} in water and 3640 ± 1620 particles kg^{-1} in sediment. Microplastic concentrations in surface waters during summer were significantly higher than in other seasons, positively linked to increased precipitation and river discharges. Polymer compositions mainly consisted of polyethylene, polypropylene, and polyethylene terephthalate, with the majority of microplastics detected smaller than 200 μm. Fragment-shaped microplastics were predominant over fibrous ones. The estimated annual input and output of microplastics through surface waters were 1.2–207 kg (2.7–150 billion particles) and 11.3–272 kg (17–769 billion particles), with the summer months contributing more than 70% of the total output. The greater microplastics output in the Jungnang Stream's waters compared to its receiving waters (Han River) indicates microplastics transport from water to other environmental compartments, such as sediments. These findings highlight the importance of investigating microplastic abundances in surface waters and sediments with temporal resolution, at least across different seasons. Such investigations offer valuable insights into the spatiotemporal occurrence and dynamic transport of microplastics, providing essential information for water management and the development of policies in freshwater ecosystems.

1. Introduction

The widespread production, usage, and uncontrolled disposal of plastics have resulted in a significant microplastic (MP) pollution issue during the last two decades (Prata, 2018). MPs, microscopic plastic debris less than 5 mm, are intentionally manufactured or generated from larger plastics (Eerkes-Medrano et al., 2015). These particles are released into the environment through anthropogenic and natural pathways, contaminating nearly all environmental media and food webs (Kwon et al., 2020; Rahman et al., 2021; Kim et al., 2022; Pham et al., 2023).

To date, research on MPs has centered on their occurrence in marine and estuarine environments (Li et al., 2018; Talbot and Chang, 2022) since oceans are accepted as ultimate sinks for MPs. However, the majority of plastic debris found in the oceans originated from terrestrial environments (Andrady, 2011; Hurley et al., 2018) whereby running freshwater bodies (e.g., streams, rivers) act as the major transport pathways (Hu et al., 2020; Rodrigues et al., 2018). The presences of MPs have primarily been explored in major rivers (Lin et al., 2024), while lower-order streams and tributaries received comparatively less attention, despite considerable concentrations of MPs in these systems (Hurley et al., 2018; Sankoda and Yamada, 2021; T.J. Park et al., 2020a). For instance, the MPs concentrations in the Han River tributaries were significantly higher than those in the river mainstem surface waters (T.J. Park et al., 2020a). Besides being transport routes, freshwater bodies can also serve as sources for MPs since some of the particles

☆ This paper has been recommended for acceptance by Eddy Y. Zeng.

* Corresponding author.
E-mail address: junghwankwon@korea.ac.kr (J.-H. Kwon).

https://doi.org/10.1016/j.envpol.2024.124362
Received 25 March 2024; Received in revised form 9 June 2024; Accepted 10 June 2024
Available online 20 June 2024
0269-7491/© 2024 Elsevier Ltd. All rights are reserved, including those for text and data mining, AI training, and similar technologies.

may deposit onto the bottom sediments. Therefore, further understanding the occurrence and dynamics of MPs in these bodies can be instrumental in addressing the expansion of inland MPs pollution into the oceans.

The analysis of both spatial and temporal distribution of MPs has gained significant attention, as these factors play a crucial role in determining the variations and transports of MPs in freshwater bodies (Talbot and Chang, 2022). Previous studies have reported the effects of anthropogenic activities, such as land cover (Carvalho et al., 2021; Grbić et al., 2020), population density (Battulga et al., 2019; Nihei et al., 2020), and wastewater treatment plants (McCormick et al., 2014) on MPs distributions. However, few studies have examined temporal variations in MPs abundances, with even fewer addressing more-than-four-season and within-wet-season variations (Eo et al., 2019). Previous studies (Eo et al., 2019; Hitchcock, 2020; Hurley et al., 2018) have reported increased MPs concentrations in waters during the wet season, whereas decreased MPs concentrations have also been observed (Barrows et al., 2018; Fan et al., 2019; Weideman et al., 2020). These findings suggested that precipitation impacts on MPs concentrations vary across different riverine systems and locations. Temporal variation of MPs in freshwater systems has been mainly investigated in larger rivers and lakes with little attention paid to smaller streams (Dikareva and Simon, 2019), although they comprise a large proportion of drainage networks. Particularly, smaller streams surrounded by populated areas may serve as crucial links between the terrestrial environments and major river networks, potentially conveying a substantial quantity of inland MPs towards the ocean. Therefore, additional research on spatiotemporal variation of MPs concentrations within

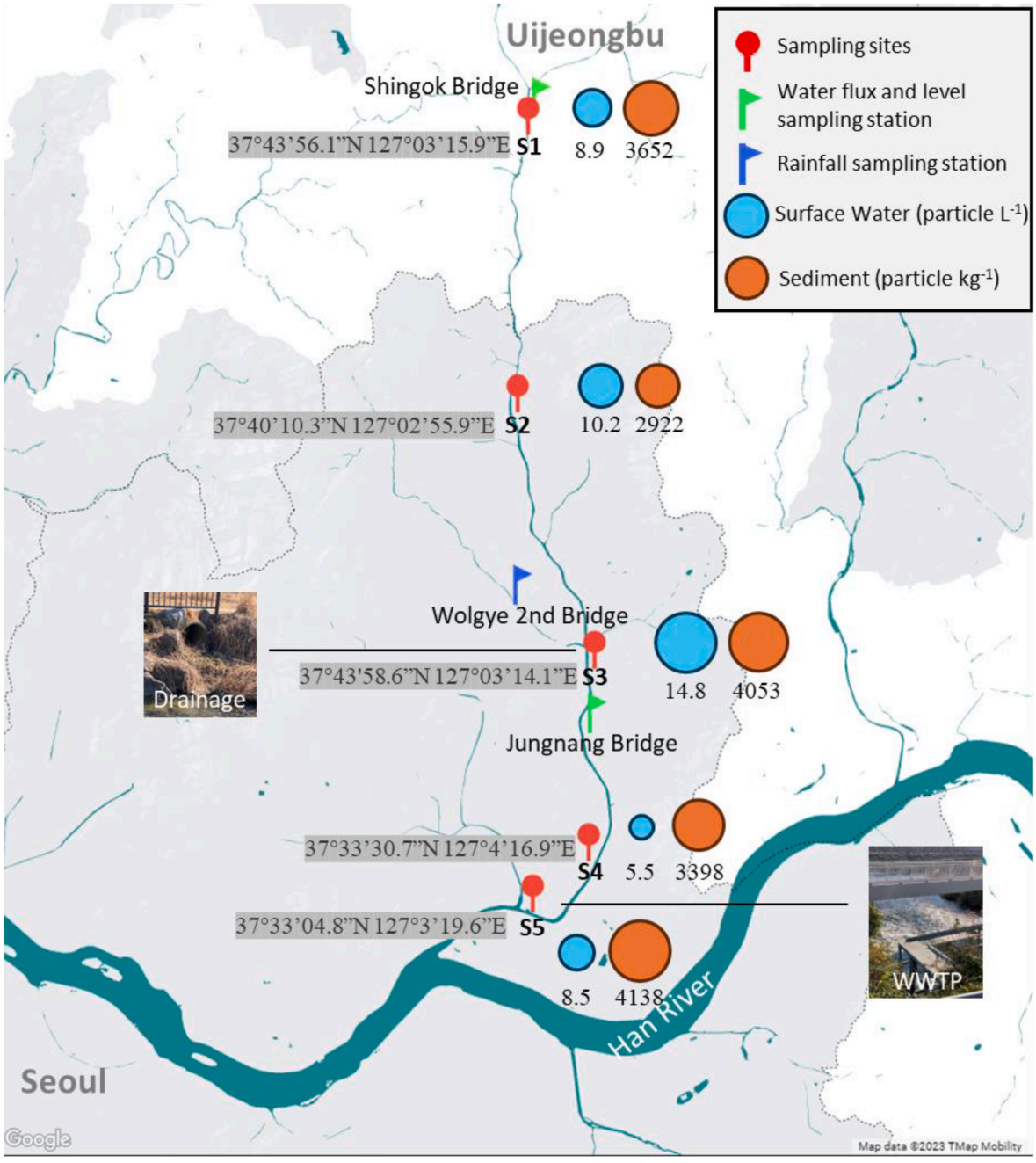

Fig. 1. Map of studied area and locations of sampling sites along the Jungnang Stream in South Korea. Average microplastics concentration in water and sediment samples are also presented.

streams is needed to better understand the spatiotemporal dynamics of MPs and their transport pathways.

This study presents a comprehensive investigation into the monthly spatiotemporal distribution of MPs in the Jungnang Stream, including their characteristics in both surface waters and sediments. Additionally, correlations between MPs abundances and temporal factors have also been explored. Furthermore, quantity of MPs input and output from the Jungnang Stream were estimated from the monthly MPs concentrations and corresponding water discharge data. To our knowledge, this is the first study to investigate the monthly spatiotemporal dynamics of MPs, down to 20 μm in size, in both surface waters and sediments within an urban stream.

2. Material and methods

2.1. Study area

The Jungnang Stream is a 37-km stream with a maximum width of 150 m and a basin area of 288 km^2. The stream is the largest tributary of the Han River, a major river flowing East-West through Seoul, the capital city of South Korea, before emptying into the Yellow Sea. The stream adjoins roads, recreational areas, residential quarters, and factories. Five sampling sites were selected along a 30 km stretch of the stream, spanning from the upstream (US) to downstream (DS) section (Fig. S1, Supplementary Material). S1 is located in the US section, while S2, S3, S4, and S5 are situated in the DS section. S3 is situated near a stormwater effluent, while a treated wastewater effluent is positioned between S4 and S5. The sampling locations are shown in Fig. 1.

2.2. Sample collection

A total of 54 water and 54 sediment samples were collected during the last week of each month from September 2021 to August 2022 (Table S1, Supplementary Material). Sampling in June was delayed to July due to a storm within the designated sampling period. Additionally, some DS samples were unattainable due to inaccessible sampling sites caused by elevated water levels during July and August. Both surface water and sediment samples were collected on the same day at each site with water samples collected before sediment samples to avoid collecting resuspended solids from sediments.

The surface water sampling method was adapted from previous studies (Eo et al., 2019; Song et al., 2018) with modifications. At each sampling site, surface waters were manually collected from the top 20 cm using 1 L clean glass beakers at five consecutive points across the stream to provide a representative sample. This yielded composite samples of 5–10 L per site, which were subsequently filtered on-site through 20 μm mesh portable nets (Fig. S2, Supplementary Material). Volume-reduced samples were obtained at the cod-end buckets of the nets and transferred to 500 mL pre-cleaned amber glass bottles. Upon arrival at the laboratory, the outside of the nets was jetted twice with water to collect any remaining particles and prevent contamination inside the nets. The two washed solutions from the cod-end buckets were then combined with the previous field-collected samples in 500 mL pre-cleaned amber glass bottles, resulting in a total volume of approximately 300 mL per water sample.

Approximately 0.5 L of wet sediment (2–5 cm depth) was collected using a grab sampling method with a stainless-steel (SUS) scoop at 3–5 consecutive points at each sampling site, following the U.S. Environmental Protection Agency sediment sampling guideline for a wadable surface water body. These samples were stored in aluminum bags and subsequently transferred to the laboratory.

2.3. Microplastic pretreatment methods

Detailed descriptions of pretreatment methods for water and sediment samples are presented in Fig. S3 and Text S1 (Supplementary Material) with sources of materials (**Text S2**). Briefly, water samples were oven dried at 70 °C until dryness, followed by the addition of 30 mL of Fenton's reagent to each sample. The samples were left at room temperature overnight (**Oxidation step**). Following organic matter digestion, MPs were density-separated by a $ZnCl_2$ solution (ρ ~1.7 g cm^{-3}) using an overflow method; After one night, the overflowed solutions were filtered through a 20 μm Anodisc, stored in clean glass petri dishes, and dried in an auto-dry desiccator for 48 h (**Separation and filtration steps**). The abundance of MPs was calculated as the number of particles per liter of water (p L^{-1}).

To extract MPs from sediments, the samples were dried at 70 °C until dryness, followed by sieving through a 2 cm pore size SUS mesh filter to remove gravel and plant residues. Sediment samples of 25–50 g were weighed into a glass flask and subjected to overnight density separation using the overflow method with the $ZnCl_2$ solution. The overflowed solution was sieved through a SUS 500 μm mesh and subsequently vacuum-filtered onto a SUS 5 μm mesh disk. Afterwards, particles on a 5 μm mesh disk underwent the same process as described in the **oxidation step** but utilizing 60 mL of Fenton reagent. After organic matter digestion, second density separation was conducted following the procedure described in the **separation and filtration steps**. The concentration of MPs was calculated as the number of particles per kilogram of dry sediment (p kg^{-1}).

2.4. Chemical and size identification

Putative MPs >500 μm were visually and tactually investigated on the SUS 500 μm filter using ultrafine forceps and a stereomicroscope, following selection criteria described by Mani et al. (2019). Suspected MPs particles were examined using an attenuated total reflection (ATR) of Integrated Infrared Imaging Microscope (FT-IR) model Thermo-Fisher Nicolet™ iN10 MX (Waltham, MA, USA).

Material compositions of MPs <500 μm were identified by Thermo-Fisher Nicolet™ iN10 MX FT-IR using the transmission mode (imaging detector). Plastic type was determined by comparing their infrared spectra to reference spectra databases. A match of 70% or more indicated a positive identification. Sizes and shapes of MPs were determined using FT-IR-microscope images and a ruler tool according to the longest dimension. Detailed FT-IR settings can be found in Table S2, Supplementary Material.

2.5. Statistical analysis

The abundances of MPs were compared spatially and temporally using two-way ANOVA. Additionally, one-way ANOVA followed by a post-hoc Tukey test, Pearson correlation coefficient, and linear regression analyses were performed to investigate any correlations of MPs concentrations between water and sediments, as well as the relationship between MPs abundances and temporal factors (Table S3, Supplementary Material). Cumulative weekly and monthly precipitation data were obtained from the Wolgye 2nd Bridge (Fig. 1), the nearest rainfall station. Daily, weekly, and monthly average discharge data of the stream were obtained from the Shingok Bridge and Jungnang Bridge stations (Fig. 1). Daily data referred to the sampling day, weekly data to the preceding week, and monthly data to the sampling month.

2.6. Calculation of annual output of microplastics through surface waters in Jungnang Stream

The input of MPs refers to the estimated quantity (number or weight) of MPs received by the Jungnang Stream from its lower tributaries in the US region, while the output denotes the estimated MPs quantity carried by the Jungnang Stream to the Han River in the DS region. To estimate the MPs input and output, monthly water flow (F) and level data (D) from the Shingok Bridge and the Jungnang Bridge stations (Table S3, Supplementary Material) were selected. These stations are the sole

sources of hydrology data for the US and DS sections of the Jungnang Stream (Han River Flood Control Office, 2023). Accordingly, MPs concentrations of water samples at S1 and S3, nearest to the Shingok Bridge and the Jungnang Bridge stations, respectively, were selected to represent input and output surface water MPs concentrations for the sampling month (C_{MPs}) (Fig. 1). A single concentration of MPs per site per month may not comprehensively represent the month-averaged MPs concentration. Nevertheless, it would be impractical to collect and analyze water and sediment samples daily or weekly along the 30-km stretch of the stream throughout the entire year. Our study improves representativeness by employing composite samples from five points per site per month, a more refined approach compared to Eo et al. (2019), averaging data from three sites per season. The calculation method was described previously by Eo et al. (2019) with modifications. A surface depth of 0.2 m was assumed, equivalent to the diameter of the sampling bottle.

$$\text{Monthly average MP input} \Big/ \text{output}\ (\text{p month}^{-1}) = \text{F}\ (\text{m}^3\ \text{s}^{-1}) \times \left(\frac{0.2\ (m)}{D\ (m)}\right) \times \text{C}_{\text{MPs}}\ (\text{p L}^{-1}) \times 1000 \quad (1)$$

The output of MPs on a weight basis (kg month^{-1}) were estimated by multiplying the monthly average MP output (p month^{-1}) through surface water by an estimated average mass of individual MP particles (AM), derived from their volume and polymer density (Pham et al., 2023). These particles were assumed to have an average spherical shape (Pham et al., 2023) and an average density (ρ) of 1.04 g mL^{-1} (Besseling et al., 2017). The geometric mean of particle size (L) was derived from log-normal distributions to minimize the influence of outliers in the dataset. The representative AM for the sampling month was calculated by averaging the monthly AMs of all DS sampling stations. The calculation method was adopted from Pham et al. (2023):

$$\text{AM}\ (\text{g}) = \frac{\pi \text{L}^3(\mu\text{m}^3) \times \rho(\text{g mL}^{-1})}{6 \times 10^{12}} \quad (2)$$

$$\text{Monthly average MP input} \Big/ \text{output}\ (\text{kg month}^{-1}) = \frac{\text{Monthly average MP input/output}\ (\text{p month}^{-1}) \times \text{AM}}{10^3} \quad (3)$$

2.7. Quality control

Laboratory apparatus and sampling nets were thoroughly cleaned, oven dried at 60 °C, and covered with aluminum foil before and after sampling. To prevent cross-contamination between sites, a different net was used at each location. Prior to analysis, pretreatment solutions and distilled water were filtered through a 0.7-μm pore size. All SUS filters were sonicated and rinsed carefully with ethanol before filtration. Organic matter digestion and density separation were carried out in the fume hood. Ethanol:H_2O (1:1 v/v) solution was used to ensure the thorough transfer of MPs between steps and eliminate potential interferences (Li et al., 2022; Obmann et al., 2018). Procedural blank samples (distilled waters) were subjected to the same analysis procedures as both waters and sediments to monitor laboratory contamination. One to five 20–100 μm MPs were found in procedural blank samples (Table S4 and S5, Supplementary Material).

Recovery tests were conducted to validate the pretreatment methods for water and sediments. Reference materials (RMs) representing four types of MPs (PE, PP, PET, and PS) were prepared. The method of producing RMs with sizes of approximately 100 μm was detailed in our previous study (Kim et al., 2022). For validation, five particles of each polymer type were spiked into 400 mL of filtered distilled water or 25 g of spare sediment samples from five sampling sites. These samples containing RMs underwent the same pretreatment and analysis methods and were repeated five times. To prevent the misidentification of environmental MPs as RMs, both FT-IR spectrum matching rates and microscope images were utilized for identification and confirmation. The RMs exhibited clear cylindrical and oval shapes with a white translucent color (Fig. S4, Supplementary Material), allowing for clear differentiation from environmental MPs.

3. Result and discussion

3.1. Method validation

The recovery rates for RMs extracted from water and sediment samples, determined after five tests, were 79 ± 6 and 81 ± 6%, respectively (Fig. S5, Supplementary Material). Specifically, in water samples, the mean recovery rates for PE, PP, PET, and PS were 80 ± 22, 88 ± 16, 72 ± 16, and 76 ± 15%, respectively. As for sediment samples, the recovery rates for PE, PP, PET, and PS were 76 ± 8, 76 ± 20, 84 ± 8, and 88 ± 16%, respectively. These recovery rates fell within an acceptable range compared to other studies (Way et al., 2022), indicating that the methods employed in this study are appropriate for investigating the numbers, sizes, and shapes of MPs in both water and sediment matrices.

3.2. Abundance and spatial distribution of MPs

The MPs (20–2000 μm) concentrations measured in water and sediment samples from five sites are presented in Fig. S6a and S6b. The MPs concentrations in water samples ranged from 1.1 to 36.4 p L^{-1} (mean 9.8 ± 7.9 p L^{-1}) (Table S4, Supplementary Material). Two-way ANOVA indicated significant difference in MPs abundance of water samples between the five sites ($p < 0.02$). Among the sites, S3 had the highest mean concentration. The gradually increased mean MPs concentrations from S1 to S3 could be potentially linked to the increased population from US to DS (Table S6, Supplementary Material) (Yan et al., 2019; Zhang et al., 2020). Subsequently, the lowest MPs concentrations were observed at sites S4 and S5 located near the stream confluence with the Han River. T.J. Park et al. (2020a) found significantly lower MPs concentrations (100–5000 μm) of 0.002 and 0.004 p L^{-1} at two Han River sampling sites closest to the stream, compared to those of S4 and S5 (100–2000 μm), suggesting a dilution effect near the

confluence.

Meanwhile, the MPs concentrations in sediment samples exhibited a wide range, from 820 to 8060 p kg^{-1} (mean 3640 ± 1620 p kg^{-1}) (Table S5, Supplementary Material). Among the sampling sites, S5 had the highest mean MPs concentration in sediments. Two-way ANOVA indicated no significant difference in MPs abundance of sediment samples between five sites. The elevated MPs concentrations observed at S3 in both water and sediment samples could be due to a stormwater drainage located before S3, discharging directly into the stream (Fig. 1). A previous study (Cho et al., 2023) observed a significantly higher MP emission via stormwater runoffs than that through the WWTP effluents in the same area in Korea, suggesting runoff as a potentially key transporter of MPs to aquatic systems. Meanwhile, the higher MPs concentrations in water and sediment at S5, compared to S4, could be attributed to the presence of smaller MPs (<100 μm) discharged from a WWTP situated between the two sites (Fig. 1) since they are more likely to pass through these facilities without filtration or settling (Simon et al., 2018). In contrast, most larger MPs (>100 μm) are effectively removed by WWTPs in Korea (H.J. Park et al., 2020). Moreover, the dominant presence of PE, PP, and PET observed in both WWTP effluences and Jungnang Stream samples supports this observation.

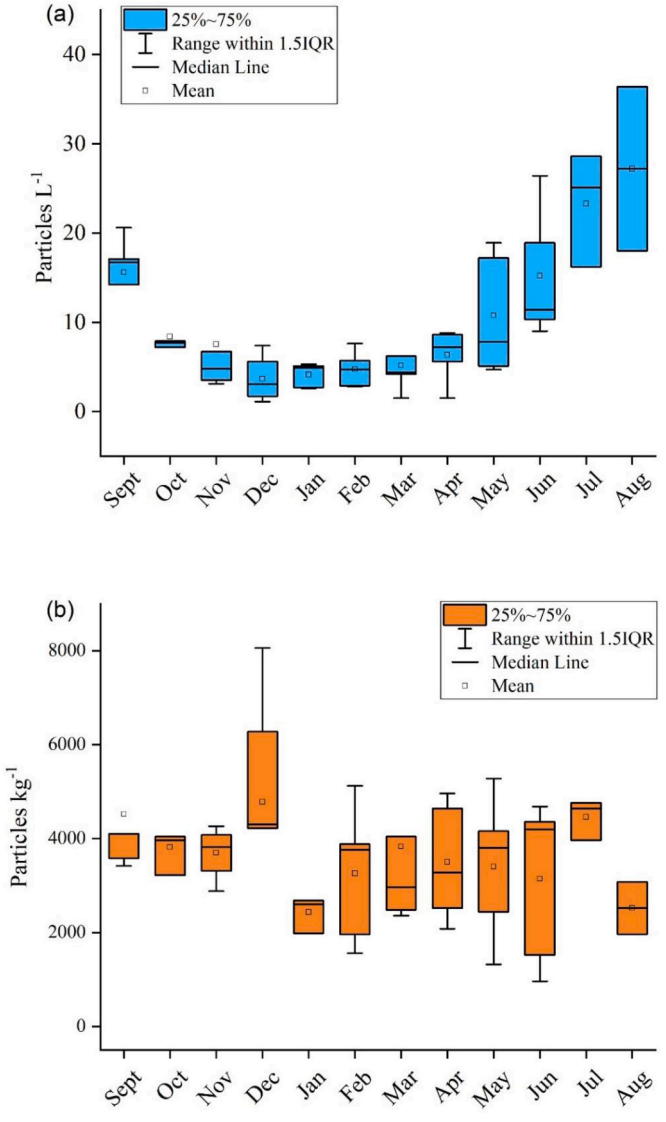

Fig. 2. Temporal distribution of microplastics in **(a)** surface water and **(b)** sediment samples. IQR: Interquartile range.

Three studies (Eo et al., 2019; T.J. Park et al., 2020a; Park et al., 2023) have monitored MP occurrences in Korean riverine systems. The mean MPs concentration in the stream water (9.8 ± 7.9 p L^{-1}) was significantly higher than those in Han River (0.007 p L^{-1}), other Han River tributaries (0.11 p L^{-1}) (T.J. Park et al., 2020a), and Nakdong River (4.8 ± 5.2 p L^{-1}) (Eo et al., 2019). Similarly, lower MPs concentrations in sediment samples of Han River (490 ± 280 p kg^{-1}) (Park et al., 2023) and Nakdong River (1970 ± 62 p kg^{-1}) (Eo et al., 2019) were observed compared to those of Jungnang Stream (3640 ± 1620 p kg^{-1}). These lower values can be explained by the exclusion of MPs (<100 μm) in Han River (T.J. Park et al., 2020a) as MPs (<100 μm) are predominant in the Jungnang Stream. The observed discrepancy in MPs concentrations between tributaries aligns with findings in a previous study (Wong et al., 2020). These variations in MPs concentrations among those water bodies can be related to the plastic (shape, size, and density) and hydrological characteristics (bed-forms, flow velocity, water-level, etc.) (Nel et al., 2018). For instance, water discharges of major rivers such as the Han River (Table S3, Supplementary Material) and Nakdong River (Eo et al., 2019) far exceed those of the Jungnang Stream, potentially leading to the lower MPs concentrations in these rivers due to dilution.

3.3. Abundance and temporal distribution of MPs

The monthly temporal variations in MPs abundances in surface waters and sediments are illustrated in Fig. 2, with details provided in Tables S1, S4, and S5 (Supplementary material). The mean MPs abundance of surface water samples ranged from 3.7 ± 2.7 (Dec) to 27 ± 13 (Aug) p L^{-1}, while the mean MPs abundance of sediments varied from 2430 ± 1180 (Jan) to 4780 ± 2630 (Dec) p kg^{-1}. The highest mean MPs concentration in waters occurred during summer (Jun–Aug), followed by autumn (Sept–Oct), spring (Mar–May), and winter (Dec–Feb) (Fig. 2a). In contrast, the mean MPs concentrations of sediments peaked during autumn, followed by spring, winter, and summer (Fig. 2b). Two-way ANOVA indicated a significant difference in both monthly ($p < 0.01$) and seasonal mean ($p < 0.01$) MPs abundance in water samples. However, no significant difference was found in either monthly or seasonal MPs abundance in sediment samples.

A more detailed assessment of seasonal dynamics was observed at S1 and S3, where monthly samples were consistently collected. Two-way ANOVA indicated a significant difference in MPs abundance in water samples between seasons ($p < 0.01$) and sites ($p < 0.02$), with no significant interactions observed between these factors. Water samples from S1 and S3 exhibited significantly higher MPs concentrations during the summer, aligning with previously documented seasonal variations in Korea and China, where precipitation peaked during summer (Eo et al., 2019; Fan et al., 2022). The summer monsoon season experiences significantly higher rainfall and faster water flow velocity compared to winter (Table S3, Supplementary Materials). Consequently, flooding events could increase the MPs influx from the land and the MPs resuspension from the sediment into the water column (Duis and Coors, 2016; Lima et al., 2015). When the river flow subsides after heavy rain, a substantial quantity of MPs in the water tends to accumulate in the sediment as temporary sinks (Free et al., 2014; Nel et al., 2018). Particularly in this study, the freezing of surface waters during winter resulted in the slowest flow rates (Table S3, Supplementary materials), potentially contributing to the highest MPs accumulation in the S1 and S3 sediments. However, no significant seasonal difference in sediment MPs concentrations was found in Jungnang Stream, in contrast to major rivers such as the Bloukrans, Han, and Liangfeng Rivers (Nel et al., 2018; Park et al., 2023; Xia et al., 2021). Since physical properties of MPs (size, shape, and composition) are similar between these aquatic bodies, other factors such as hydrological characteristics and watershed patterns can be crucial in governing the deposition and transport of MPs in sediments (Kumar et al., 2021), necessitating further research. Additionally, the significant increase in water MPs concentrations during summer

suggests that stormwater runoff and WWTPs may serve as predominant sources of MPs in waters compared to suspension of MPs in sediments.

3.4. Correlations between microplastic concentrations and temporal variables

MPs concentrations between wet and dry seasons are commonly observed in surface waters, these patterns may not necessarily apply to MPs in sediments (Talbot and Chang, 2022). This could be attributed to the more intense MPs fluctuations in surface water, while MPs tend to accumulate and persist in sediments for longer periods, representing more long-term concentrations (Ding et al., 2019). Consequently, it is common for studies to report a lack of correlations or disproportional abundance between surface water and sediment samples (Talbot and Chang, 2022). This study also found no significant correlation between MPs in water and sediment samples.

Weekly accumulated precipitation showed an average weak correlation with MPs concentrations in both water and sediment (Table S7, Supplementary Material) at all sites. Meanwhile, monthly accumulated precipitation exhibited a weak relationship with sediment MPs abundances but a positively significant linear correlation with water sample MPs abundances ($r > 0.71$, $p < 0.03$), except for S4 and S5 (Table S7 and Fig. S7a, Supplementary Material). The results of this study are consistent with previous studies (Cao et al., 2023; Wong et al., 2020; Xia et al., 2020) conducted in Northeast Asia that possibly have similar wet-dry seasons. Meanwhile, the lack of correlation between monthly precipitation and MPs concentrations at S4 and S5 may result from MPs concentrations being more heavily influenced by anthropogenic than environmental variables (Mani and Burkhardt-Holm, 2020), or MPs concentrations varying more strongly as a function of spatial rather than temporal factors (Mintenig et al., 2020). For instance, possible dilution occurred in the stream confluence with the Han River (T.J. Park et al., 2020a) and the release of WWTP effluent (Tien et al., 2020) might mitigate the impacts of precipitation on MPs concentrations at these sites. Moreover, the absence of MPs data at S4 and S5 during summer could also contribute to this lack of correlation.

Similar trends were observed between MPs concentrations at S1 and S3 and river discharges collected near these sites (Table S7 and Fig. S7b, Supplementary Material). Only monthly discharges exhibited a positively significant linear correlation with water sample MPs abundances at ($r > 0.71$, $p < 0.01$). Evidence of positive correlations between MPs concentrations and water discharge has been reported in previous studies (Carvalho et al., 2021; Tien et al., 2020; Wagner et al., 2019). These findings indicate that streams serve as significant conduits for the transport of terrestrial and airborne MPs into rivers, especially during flood events (Bergmann et al., 2019, 2017). Further research is needed to understand the contributions of transport pathways of MPs, such as through runoff during rain events, to MPs contaminations in riverine systems.

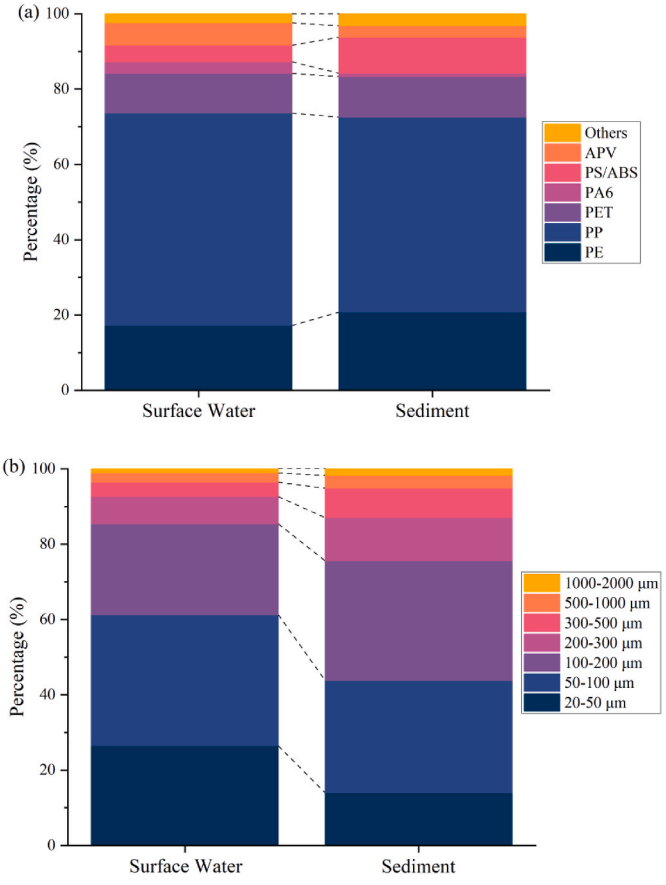

Fig. 3. (a) Microplastic compositions and **(b)** size distribution in surface water and sediment samples. APV: acrylates/polyurethanes/varnish cluster; PS: polystyrene; ABS: acrylonitrile butadiene styrene; PA: polyamide; PET: polyethylene terephthalate; PP: polypropylene; PE: polyethylene.

3.5. Microplastic compositions, sizes, and shapes

Fig. 3a presents the polymer type distribution of MPs in water and sediment samples. The predominant polymer types identified in both water and sediment samples were PE, PP, and PET (Tables S4 and S5, Supplementary Material), consistent with results from other studies (Park et al., 2023, T.J. Park et al., 2020a). These polymers are widely used in daily life (plastic bags, mulches, packaging, etc.) due to their low weight and stability (PlasticsEurope, 2021). Among them, PP exhibited the highest spatial and temporal prevalence across all samples. The average proportional composition of MPs was largely similar between water and sediment samples, possibly due to the shallow depth at the sampling sites (Table S3, Supplementary Material). The occurrence of low-density particles (<1 g cm^{-1}) in sediments can be attributed to their enhanced settling facilitated by biofilm development (Lee et al., 2022), while high-density MPs (>1 g cm^{-1}) can re-suspend from sediments to water columns during flood events. This is supported by their predominant presence in waters and minimal occurrence in sediments during summer.

A majority of MPs detected in all samples were smaller than 200 µm (67.4–92.2%) (Fig. 3b). Overall, 50–100 µm MP were predominant in water samples (29.1–44.8%), while the predominant size range was 100–200 µm (28–45.4%) in sediments. The higher proportion of 100–200 µm MP than 50–100 µm MP in sediments can be linked to their enhanced settling with increasing particle size (Lee et al., 2022). Furthermore, reduced rainfall and flow velocity during winter facilitated the deposition of the bigger MPs from waters to sediments, leaving a higher proportion of smaller MPs (20–50 µm) in waters during summer, consistent with findings from previous studies (Carvalho et al., 2021; Tien et al., 2020). Two main shapes of MPs were identified: fibers and fragments. On average, fragments accounted for a higher proportion (63.2%–96.9%) compared to fibers (3.1%–36.8%) (Fig. S8, Supplementary Material) in both waters and sediments. This indicates that most of the MPs in the stream are secondary in origin (Cole et al., 2011). However, increased fibrous MPs, especially PET, were observed in waters and sediments during the wet season (Table S4 and S5, Supplementary Material), possibly due to stormwater run-off, WWTPs, and atmospheric deposition (Cai et al., 2017; Fisher et al., 2016). Previous studies (Park et al., 2023; T.J. Park et al., 2020a, b) also reported that greater than 73% of MPs in Korean riverine systems were fragments. The results indicate a direct correlation in the shape patterns of MPs between the Han River and its tributaries, while in other countries (Su et al., 2016; Rodrigues et al., 2018; Wang et al., 2017), fibers are the most abundant type, implying that the MPs shape varied between different

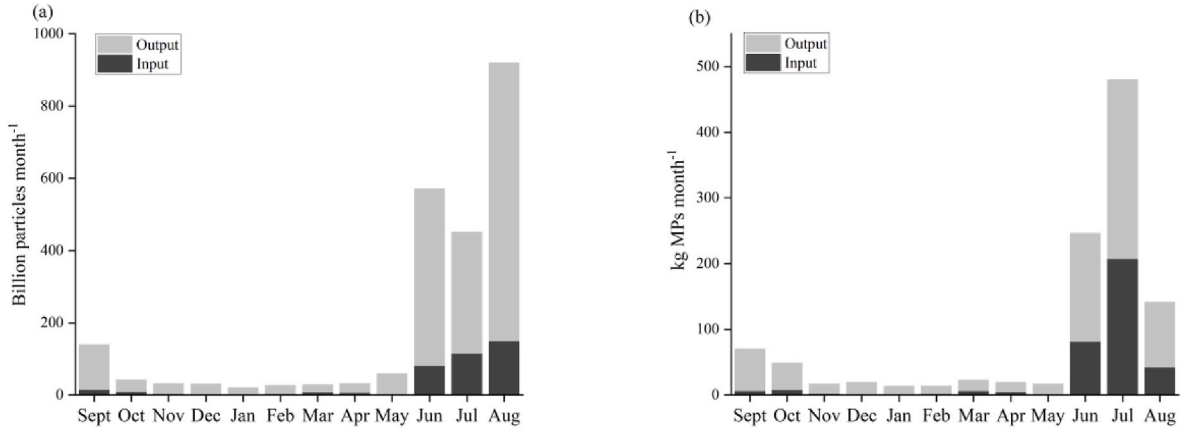

Fig. 4. Monthly input and output of microplastics carried by the Jungnang Stream surface waters by **(a)** number and **(b)** weight.

locations.

3.6. Annual input and output of microplastics through the surface water in the Jungnang Stream

Potential transport pathways and sources of MPs along the stream were illustrated in Fig. S9 (Supplementary Material). The monthly US MPs input ranged from 1.2 to 207 kg (2.7–150 billion particles), while the monthly DS MPs output varied between 11.3 and 272 kg (17–769 billion particles) (Fig. 4a and b). Both inputs and outputs peaked during summer and were lowest during winter, reflecting significant seasonal variations. This highlights the importance of considering temporal resolutions, at least across different seasons, when estimating the annual MPs output, as relying on data from one season may lead to inaccurate estimations. Moreover, the outputs were consistently higher than the inputs each month (Table S6, Supplementary Material), indicating contributions of MPs from other sources along the river (e.g., tributaries, WWTPs, stormwater, etc.). As stormwater runoff is a critical pathway for MPs, measures, such as passive physical filtration systems during floods, can significantly reduce the MPs influx MPs into the ocean.

The estimated total annual input and output of MPs through the surface waters were 0.37 tons year^{-1} (0.4 trillion particle year^{-1}) and 0.74 tons year^{-1} (2.0 trillion particle year^{-1}), respectively (Fig. 4b). The three summer months (Jun–Aug) accounted for 81.9% of the total number and 72.3% of the total weight of the estimated annual output (Table S6, Supplementary Material). Increased precipitation rates were correlated with the predominant input and output during summer. Additionally, if C_{MPs} of surface water is assumed to represent the average vertical concentration of MPs in the water column, the estimated total output of MPs (surface and subsurface water) would be 2.6 tons year^{-1} (7.5 trillion particle year^{-1}). The total output of MPs per population density throughout vertical water columns was 161.6 g km^2 capita^{-1} year^{-1} (469 million particle km^2 capita^{-1} year^{-1}), significantly lower than 195 kg km^2 capita^{-1} year^{-1} (17.9 billion particle km^2 capita^{-1} year^{-1}) reported by Eo et al. (2019), primarily due to the higher total MPs output and lower population density around the Nakdong River.

To assess the contribution of MPs from the Jungnang Stream to the overall output of MPs in the Han River, the number and weight of MPs output in the Han River were estimated based on MPs concentrations and size distributions at the sampling site H7 (closest to the Jungnang Stream) in a previous study (T.J. Park et al., 2020a). Consequently, the estimated MPs output in the Han River was 11.0 tons year^{-1} (0.9 trillion particle year^{-1}). Considering the exclusion of MPs <100 μm by T.J. Park et al. (2020a), the revised estimate for MPs transported from the Jungnang Stream to the Han River was 19.3 tons year^{-1} (3.2 trillion particles year^{-1}). The higher MPs output in stream's waters compared to the Han River suggests significant MP transport from waters of the Han River to other environmental compartments. For instance, the greater depth of the Han River at Hangang Bridge station (62–236 cm) (Table S8, Supplementary Material) may result in a lower flow rate at the riverbed, promoting MP accumulation in sediments and restricting resuspension. This suggests a more stable accumulation of MPs in the Han River sediments. The substantially higher MPs concentrations in waters at depths greater than 2 m (60 p m^{-3}), compared to the surface water (<2 m) (2.4 p m^{-3}) of the Han River further support the downward movement of MPs within the river (T.J. Park et al., 2020a). In contrast, the shallower depth of the Jungnang Stream (less than 1 m) facilitates resuspension of MPs from sediments to surface waters, leading to a higher output. Although assuming representative MPs in the Jungnang Stream is reasonable due to its shallow depth and lower vertical heterogeneity, estimating MPs for an entire stream based solely on surface water data may result in under- or overestimation of the output. Furthermore, the waters in the Han River sampled by T.J. Park et al. (2020a) were obtained only once, and the seasonal context of the sampling is unknown, restricting the precise comparison of MP outputs between the two water bodies. Thus, it is recommended to acquire a vertical profile of microplastic abundance with higher spatial and temporal resolution to better understand the MPs transport between water bodies and achieve a more realistic estimate of the annual MPs output delivered to the ocean.

4. Conclusion

The monthly spatiotemporal distribution and characteristics of MPs in both surface water and sediment were investigated along the Jungnang Stream in Korea. The concentrations of MPs in surface water and sediment samples ranged from 1.1 to 36.4 p L^{-1} and from 820 to 8060 p kg^{-1}, respectively. Seasonal trends showed higher mean MPs concentrations during summer in water samples, but during autumn in sediment samples. Positive linear correlations were found between MPs concentrations in surface waters and monthly accumulated precipitations or average flow rates. Consequently, concentrated rainfalls during the monsoon season play a crucial role in transporting terrestrial and airborne MPs into riverine systems. The predominant polymer compositions identified were PE, PP, and PET, with most MPs being smaller than 200 μm (67.4–92.2%). The estimated annual input and output of MPs through surface waters were 1.2–207 kg (2.7–150 billion particles) and 11.3–272 kg (17–769 billion particles), with the summer months contributing over 70% to the total input and output. The findings suggest that measures should be specifically targeted during rainfalls to effectively reduce the transport of MPs into the ocean. The greater MPs output in the Jungnang Stream compared to the Han River indicates substantial MP transport from water to other environmental compartments, such as sediment accumulation. This study extends the understanding of the occurrence and spatiotemporal dynamics of MPs in

freshwater for the further development of water management and policy.

CRediT authorship contribution statement

Dat Thanh Pham: Writing – original draft, Visualization, Validation, Methodology, Investigation, Conceptualization. **Sang-Hyun Choi:** Methodology, Data curation. **Jung-Hwan Kwon:** Writing – review & editing, Supervision, Funding acquisition, Conceptualization.

Declaration of competing interest

The authors declare that they have no known competing financial interests or personal relationships that could have appeared to influence the work reported in this paper.

Data availability

Data will be made available on request.

Acknowledgement

This work was supported by a National Research Foundation of Korea (NRF) grant funded by the Korean Government (Ministry of Science and ICT) (No. RS-2023-00209242) and the BK21 FOUR program (Grant No. 4120200313708) funded by National Research Foundation of Korea (NRF).

Appendix A. Supplementary data

Supplementary data to this article can be found online at https://doi.org/10.1016/j.envpol.2024.124362.

References

Andrady, A.L., 2011. Microplastics in the marine environment. Mar. Pollut. Bull. 62 (8), 1596–1605. https://doi.org/10.1016/j.marpolbul.2011.05.030.

Barrows, A.P.W., Christiansen, K.S., Bode, E.T., Hoellein, T.J., 2018. A watershed-scale, citizen science approach to quantifying microplastic concentration in a mixed land-use river. Water Res. 147, 382–392. https://doi.org/10.1016/j.watres.2018.10.013.

Battulga, B., Kawahigashi, M., Oyuntsetseg, B., 2019. Distribution and composition of plastic debris along the river shore in the Selenga River basin in Mongolia. Environ. Sci. Pollut. Res. 26, 14059–14072. https://doi.org/10.1007/s11356-019-04632-1.

Bergmann, M., Lutz, B., Tekman, M.B., Gutow, L., 2017. Citizen scientists reveal: marine litter pollutes Arctic beaches and affects wild life. Mar. Pollut. Bull. 125, 535–540. https://doi.org/10.1016/j.marpolbul.2017.09.055.

Bergmann, M., Mützel, S., Primpke, S., Tekman, M.B., Trachsel, J., Gerdts, G., 2019. White and wonderful? Microplastics prevail in snow from the Alps to the Arctic. Sci. Adv. 5, 1–11. https://doi.org/10.1126/sciadv.aax1157.

Besseling, E., Quik, J.T.K., Sun, M., Koelmans, A.A., 2017. Fate of nano- and microplastic in freshwater systems: a modeling study. Environt. Pollut. 220, 540–548. https://doi.org/10.1016/j.envpol.2016.10.001.

Cai, L., Wang, J., Peng, J., Tan, Z., Zhan, Z., Tan, X., Chen, Q., 2017. Characteristic of microplastics in the atmospheric fallout from Dongguan city, China: preliminary research and first evidence. Environ. Sci. Pollut. Res. 24, 24928–24935. https://doi.org/10.1007/s11356-017-0116-x.

Cao, L., Chen, W., Wang, Y., Li, S., Jin, Z., Bian, J., Li, Q., Li, M., 2023. Temporal and spatial distribution characteristics of microplastics and their influencing factors in the lincheng river, zhoushan city, China. Processes 11 (4), 1136. https://doi.org/10.3390/pr11041136.

Cho, Y., Shim, W.J., Ha, S.Y., Han, G.M., Jang, M., Hong, S.H., 2023. Microplastic emission characteristics of stormwater runoff in an urban area: intra-event variability and influencing factors. Sci. Total Environ. 866, 161318 https://doi.org/10.1016/j.scitotenv.2022.161318.

Carvalho, A.R., Garcia, F., Riem-Galliano, L., Tudesque, L., Albignac, M., ter Halle, A., Cucherousset, J., 2021. Urbanization and hydrological conditions drive the spatial and temporal variability of microplastic pollution in the Garonne River. Sci. Total Environ. 769, 144479 https://doi.org/10.1016/j.scitotenv.2020.144479.

Cole, M., Lindeque, P., Halsband, C., Galloway, T.S., 2011. Microplastics as contaminants in the marine environment: a review. Mar. Pollut. Bull. 62, 2588–2597. https://doi.org/10.1016/j.marpolbul.2011.09.025.

Dikareva, N., Simon, K.S., 2019. Microplastic pollution in streams spanning an urbanisation gradient. Environ. Pollut. 250, 292–299. https://doi.org/10.1016/j.envpol.2019.03.105.

Ding, L., Mao, R. fan, Guo, X., Yang, X., Zhang, Q., Yang, C., 2019. Microplastics in surface waters and sediments of the Wei River, in the northwest of China. Sci. Total Environ. 667, 427–434. https://doi.org/10.1016/j.scitotenv.2019.02.332.

Duis, K., Coors, A., 2016. Microplastics in the aquatic and terrestrial environment: sources (with a specific focus on personal care products), fate and effects. Environ. Sci. Eur. 28, 2. https://doi.org/10.1186/s12302-015-0069-y.

Eerkes-Medrano, D., Thompson, R.C., Aldridge, D.C., 2015. Microplastics in freshwater systems: a review of the emerging threats, identification of knowledge gaps and prioritisation of research needs. Water Res. 75, 63–82. https://doi.org/10.1016/j.watres.2015.02.012.

Eo, S., Hong, S.H., Song, Y.K., Han, G.M., Shim, W.J., 2019. Spatiotemporal distribution and annual load of microplastics in the Nakdong River, South Korea. Water Res. 160, 228–237. https://doi.org/10.1016/j.watres.2019.05.053.

Fan, Y., Zheng, J., Deng, L., Rao, W., Zhang, Q., Liu, T., Qian, X., 2022. Spatiotemporal dynamics of microplastics in an urban river network area. Water Res. 212, 118116 https://doi.org/10.1016/j.watres.2022.118116.

Fan, Y., Zheng, K., Zhu, Z., Chen, G., Peng, X., 2019. Distribution, sedimentary record, and persistence of microplastics in the Pearl River catchment, China. Environ. Pollut. 251, 862–870. https://doi.org/10.1016/j.envpol.2019.05.056.

Fisher, E.K., Paglialonga, L., Czech, E., Tamminga, M., 2016. Microplastic pollution in lakes and lake shoreline sediments - a case study on Lake Bolsena and Lake Chiusi (central Italy). Environ. Pollut. 213, 648–657. https://doi.org/10.1016/j.envpol.2016.03.012.

Free, C.M., Jensen, O.P., Mason, S.A., Eriksen, M., Williamson, N.J., Boldgiv, B., 2014. High-levels of microplastic pollution in a large, remote, mountain lake. Mar. Pollut. Bull. 85, 156–163. https://doi.org/10.1016/j.marpolbul.2014.06.001.

Grbić, J., Helm, P., Athey, S., Rochman, C.M., 2020. Microplastics entering northwestern Lake Ontario are diverse and linked to urban sources. Water Res. 174, 115623 https://doi.org/10.1016/j.watres.2020.115623.

Han River Flood Control Office, 2023. Water resources management information system. http://wamis.go.kr/.

Hitchcock, J.N., 2020. Storm events as key moments of microplastic contamination in aquatic ecosystems. Sci. Total Environ. 734, 139436 https://doi.org/10.1016/j.scitotenv.2020.139436.

Hu, D., Zhang, Y., Shen, M., 2020. Investigation on microplastic pollution of Dongting Lake and its affiliated rivers. Mar. Pollut. Bull. 160, 111555 https://doi.org/10.1016/j.marpolbul.2020.111555.

Hurley, R., Woodward, J., Rothwell, J.J., 2018. Microplastic contamination of river beds significantly reduced by catchment-wide flooding. Nat. Geosci. 11, 251–257. https://doi.org/10.1038/s41561-018-0080-1.

Kim, J., Pham, D.T., Park, H.J., Chae, M.Y, Lee, S.H., Hong, S., Kim, J.Y., Jung, J., Lee, B. T., Kwon, J.H., 2022. Development and validation of analytical methods for detecting and identifying microplastics in salts, soy sauce, and salted pollock roe. J. Food Compos. Anal. 114, 104856 https://doi.org/10.1016/j.jfca.2022.104856.

Kumar, R., Sharma, P., Verma, A., Jha, P.K., Singh, P., Gupta, P.K., Chandra, R., Vara Prasad, P.V., 2021. Effect of physical characteristics and hydrodynamic conditions on transport and deposition of microplastics in riverine ecosystem. Water 13 (19), 2710. https://doi.org/10.3390/w13192710.

Kwon, J.H., Kim, J.W., Pham, T.D., Tarafdar, A., Hong, S., Chun, S.H., Lee, S.H., Kang, D. Y., Kim, J.Y., Kim, S. Bin, Jung, J., 2020. Microplastics in food: a review on analytical methods and challenges. Int. J. Environ. Res. Public Health 17, 1–23. https://doi.org/10.3390/ijerph17186710.

Lee, S.Y., An, J., Kim, J., Kwon, J.H., 2022. Enhanced settling of microplastics after biofilm development: a laboratory column study mimicking wastewater clarifiers. Environ. Pollut. 311, 119909 https://doi.org/10.1016/j.envpol.2022.119909.

Li, D., Sheerin, E.D., Shi, Y., Xiao, L., Yang, L., Boland, J.J., Wang, J.J., 2022. Alcohol pretreatment to eliminate the interference of micro additive particles in the identification of microplastics using Raman spectroscopy. Environ. Sci. Technol. 56 (17), 12158–12168. https://doi.org/10.1021/acs.est.2c01551.

Li, J., Liu, H., Paul Chen, J., 2018. Microplastics in freshwater systems: a review on occurrence, environmental effects, and methods for microplastics detection. Water Res. 137, 362–374. https://doi.org/10.1016/j.watres.2017.12.056.

Lima, A.R.A., Barletta, M., Costa, M.F., 2015. Seasonal distribution and interactions between plankton and microplastics in a tropical estuary. Estuar. Coast Shelf Sci. 165, 213–225. https://doi.org/10.1016/j.ecss.2015.05.018.

Lin, H.T., Schneider, F., Aziz, M.A., Wong, K.Y., Arunachalam, K.D., Praveena, S.M., Sethupathi, S., Chong, W.C., Nafisyah, A.L., Parthasarathy, P., Chelliapan, S., Kunz, A., 2024. Microplastics in Asian rivers: geographical distribution, most detected types, and inconsistency in methodologies. Environ. Pollut. 349, 123985 https://doi.org/10.1016/j.envpol.2024.123985.

Mani, T., Burkhardt-Holm, P., 2020. Seasonal microplastics variation in nival and pluvial stretches of the Rhine River - from the Swiss catchment towards the North Sea. Sci. Total Environ. 707, 135579 https://doi.org/10.1016/j.scitotenv.2019.135579.

Mani, T., Primpke, S., Lorenz, C., Gerdts, G., Burkhardt-Holm, P., 2019. Microplastic pollution in benthic midstream sediments of the rhine river. Environ. Sci. Technol. 53, 6053–6062. https://doi.org/10.1021/acs.est.9b01363.

McCormick, A., Hoellein, T.J., Mason, S.A., Schluep, J., Kelly, J.J., 2014. Microplastic is an abundant and distinct microbial habitat in an urban river. Environ. Sci. Technol. 48, 11863–11871. https://doi.org/10.1021/es503610r.

Mintenig, S.M., Kooi, M., Erich, M.W., Primpke, S., Redondo- Hasselerharm, P.E., Dekker, S.C., Koelmans, A.A., van Wezel, A.P., 2020. A systems approach to understand microplastic occurrence and variability in Dutch riverine surface waters. Water Res. 176, 115723 https://doi.org/10.1016/j.watres.2020.115723.

Nel, H.A., Dalu, T., Wasserman, R.J., 2018. Sinks and sources: assessing microplastic abundance in river sediment and deposit feeders in an Austral temperate urban river

system. Sci. Total Environ. 612, 950–956. https://doi.org/10.1016/j.scitotenv.2017.08.298.
Nihei, Y., Yoshida, T., Kataoka, T., Ogata, R., 2020. High-Resolution mapping of Japanese microplastic and macroplastic emissions from the land into the sea. Water 12 (4), 951. https://doi.org/10.3390/W12040951.
Obmann, B., Sarau, G., Holtmannspotter, H., Pischetsrieder, M., Christiansen, S.H., Dicke, W., 2018. Small-sized microplastics and pigmented particles in bottled mineral water. Water Res. 141, 307–316. https://doi.org/10.1016/j.watres.2018.05.027.
Park, H.J., Oh, M.J., Kim, P.G., Kim, G., Jeong, D.H., Ju, B.K., Lee, W.S., Chung, H.M., Kang, H.J., Kwon, J.H., 2020. National reconnaissance survey of microplastics in municipal wastewater treatment plants in Korea. Environ. Sci. Technol. 54, 1503–1512. https://doi.org/10.1021/acs.est.9b04929.
Park, T.J., Kim, M.K., Lee, S.H., Kim, M.J., Lee, Y.S., Lee, B.M., Seong, K.S., Park, J.H., Zoh, K.D., 2023. Temporal and spatial distribution of microplastic in the sediment of the Han River, South Korea. Chemosphere 317, 137831. https://doi.org/10.1016/j.chemosphere.2023.137831.
Park, T.J., Lee, Seung Hyun, Lee, M.S., Lee, J.K., Lee, Soo Hyung, Zoh, K.D., 2020a. Occurrence of microplastics in the Han River and riverine fish in South Korea. Sci. Total Environ. 708, 134535 https://doi.org/10.1016/j.scitotenv.2019.134535.
Park, T.J., Lee, S.H., Lee, M.S., Lee, J.K., Park, J.H., Zoh, K.D., 2020b. Distribution of microplastics in surface water, fish, and sediment in the vicinity of a sewage treatment plant. Water 12, 3333. https://doi.org/10.3390/w12123333.
Pham, D.T., Kim, J., Lee, S.H., Kim, J., Kim, D., Hong, S., Jung, J., Kwon, J.H., 2023. Analysis of microplastics in various foods and assessment of aggregate human exposure via food consumption in Korea. Environ. Pollut. 322, 121153 https://doi.org/10.1016/j.envpol.2023.121153.
PlasticsEurope, 2021. Plastcs-the facts 2021: an analysis of European plastics production. Demand, and Waste Data 1–34.
Prata, J.C., 2018. Airborne microplastics: consequences to human health? Environ. Pollut. 234, 115–126. https://doi.org/10.1016/j.envpol.2017.11.043.
Rahman, A., Sarkar, A., Yadav, O.P., Achari, G., Slobodnik, J., 2021. Potential human health risks due to environmental exposure to nano- and microplastics and knowledge gaps: a scoping review. Sci. Total Environ. 757, 143872 https://doi.org/10.1016/j.scitotenv.2020.143872.
Rodrigues, M.O., Abrantes, N., Gonçalves, F.J.M., Nogueira, H., Marques, J.C., Gonçalves, A.M.M., 2018. Spatial and temporal distribution of microplastics in water and sediments of a freshwater system (Antuã River, Portugal). Sci. Total Environ. 633, 1549–1559. https://doi.org/10.1016/j.scitotenv.2018.03.233.
Sankoda, K., Yamada, Y., 2021. Occurrence, distribution, and possible sources of microplastics in the surface river water in the Arakawa River watershed. Environ. Sci. Pollut. 28, 27474–27480. https://doi.org/10.1007/s11356-021-12459-y.
Simon, M., Alst, N., Vollertsen, J., 2018. Quantification of microplastic mass and removal rates at wastewater treatment plants applying Focal Plane Array (FPA)-based Fourier Transform Infrared (FT-IR) imaging. Water Res. 142, 1–9. https://doi.org/10.1016/j.watres.2018.05.019.
Song, Y.K., Hong, S.H., Eo, S., Jang, M., Han, G.M., Isobe, A., Shim, W.J., 2018. Horizontal and vertical distribution of microplastics in Korean coastal waters. Environ. Sci. Technol. 52, 12188–12197. https://doi.org/10.1021/acs.est.8b04032.
Su, L., Xue, Y., Li, L., Yang, D., Kolandhasamy, P., Li, D., Shi, H., 2016. Microplastics in taihu lake, China. Environ. Pollut. 216, 711–719. https://doi.org/10.1016/j.envpol.2016.06.036.
Talbot, R., Chang, H., 2022. Microplastics in freshwater: a global review of factors affecting spatial and temporal variations. Environt. Pollut. 292, 118393 https://doi.org/10.1016/j.envpol.2021.118393.
Tien, C.J., Wang, Z.X., Chen, C.S., 2020. Microplastics in water, sediment and fish from the Fengshan River system: relationship to aquatic factors and accumulation of polycyclic aromatic hydrocarbons by fish. Environ. Pollut. 265, 114962 https://doi.org/10.1016/j.envpol.2020.114962.
Wagner, S., Klöckner, P., Stier, B., Römer, M., Seiwert, B., Reemtsma, T., Schmidt, C., 2019. Relationship between discharge and river plastic concentrations in a rural and an urban catchment. Environ. Sci. Technol. 53, 10082–10091. https://doi.org/10.1021/acs.est.9b03048.
Wang, W., Ndungu, A.W., Li, Z., Wang, J., 2017. Microplastics pollution in inland freshwaters of China: a case study in urban surface waters of Wuhan. China. Sci. Total Environ. 575, 1369–1374. https://doi.org/10.1016/j.scitotenv.2016.09.213.
Way, C., Hudson, M.D., Williams, I.D., Langley, G.J., 2022. Evidence of underestimation in microplastic research: a meta-analysis of recovery rate studies. Sci. Total Environ. 805, 150227 https://doi.org/10.1016/j.scitotenv.2021.150227.
Weideman, E.A., Perold, V., Ryan, P.G., 2020. Limited long-distance transport of plastic pollution by the Orange-Vaal River system, South Africa. Sci. Total Environ. 727, 138653 https://doi.org/10.1016/j.scitotenv.2020.138653.
Wong, G., Löwemark, L., Kunz, A., 2020. Microplastic pollution of the Tamsui River and its tributaries in northern Taiwan: spatial heterogeneity and correlation with precipitation. Environ. Pollut. 260, 1–12. https://doi.org/10.1016/j.envpol.2020.113935.
Xia, F., Yao, Q., Zhang, J., Wang, D., 2021. Effects of seasonal variation and resuspension on microplastics in river sediments. Environ. Pollut. 286, 117403 https://doi.org/10.1016/j.envpol.2021.117403.
Xia, W., Rao, Q., Deng, X., Chen, J., Xie, P., 2020. Rainfall is a significant environmental factor of microplastic pollution in inland waters. Sci. Total Environ. 732, 139065 https://doi.org/10.1016/j.scitotenv.2020.139065.
Yan, M., Nie, H., Xu, K., He, Y., Hu, Y., 2019. Chemosphere microplastic abundance, distribution and composition in the pearl river along guangzhou city and pearl river estuary, China. Chemosphere 217, 879–886. https://doi.org/10.1016/j.chemosphere.2018.11.093.
Zhang, Y., Kang, S., Allen, S., Allen, D., Gao, T., 2020. Earth-Science Reviews Atmospheric microplastics: a review on current status and perspectives. Earth Sci. Rev. 203, 103118 https://doi.org/10.1016/j.earscirev.2020.103118.